

Bilateral prefrontal cortex oxygenation responses to a verbal fluency task: a multichannel time-resolved near-infrared topography study

Valentina Quaresima

Marco Ferrari

University of L'Aquila
Department of Biomedical Sciences and Technologies
I-67100 L'Aquila, Italy

Alessandro Torricelli

Lorenzo Spinelli

Antonio Pifferi

Rinaldo Cubeddu

Politecnico di Milano
INFN-Dipartimento di Fisica and IFN-CNR
Piazza Leonardo da Vinci 32
20133 Milan, Italy

Abstract. The letter-fluency task-induced response over the prefrontal cortex is investigated bilaterally on eight subjects using a recently developed compact, eight-channel, time-resolved, near-IR system. The cross-subject mean values of prefrontal cortex oxygen saturation (SO_2) were $68.8 \pm 3.2\%$ (right) and $71.0 \pm 3.6\%$ (left), and of total hemoglobin concentration (tHb) were $69.6 \pm 9.6 \mu M$ (right) and $69.5 \pm 9.9 \mu M$ (left). The typical cortical activation response to the cognitive task [characterized by an increase in oxyhemoglobin (O_2Hb) with a concurrent decrease in deoxyhemoglobin (HHb)] at each measurement point is observed in only four subjects. In this subset, the amplitude of the O_2Hb increase and HHb decrease is uniform over each prefrontal cortex area and comparable between the two hemispheres. These findings agree with previous studies using continuous wave functional near-IR spectroscopy and functional magnetic resonance imaging, therefore demonstrating the potential of a time-resolved spectroscopy approach. In addition, a significant increase in SO_2 levels was observed in the right ($1.1 \pm 0.5\%$) compared to left side of the prefrontal cortex ($0.9 \pm 0.5\%$) ($P = 0.005$). A different pattern of cortical activation (characterized by the lack of HHb decrease or even increased HHb) was observed in the remaining subjects. © 2005 Society of Photo-Optical Instrumentation Engineers. [DOI: 10.1117/1.1851512]

Keywords: near-infrared spectroscopy; time-resolved spectroscopy; brain; verbal fluency task; cortical activation.

Paper NEU-04 received Mar. 1, 2004; revised manuscript received May 1, 2004; accepted for publication May 17, 2004; published online Feb. 1, 2005.

1 Introduction

Starting almost 27 years ago with the pioneering work of Jobsis,¹ noninvasive near-IR spectroscopy (NIRS) was initially employed to investigate brain oxygenation in neonates and adults both experimentally and clinically, and later to assess muscle oxidative metabolism in pathophysiology (for reviews see Refs. 2–4). In spite of the powerful, high-cost tools for human brain mapping such as positron emission tomography (PET) and functional magnetic resonance imaging (fMRI), since 1993,^{5–7} functional NIRS (fNIRS) using a continuous wave (cw) has been largely used to investigate functional activation of the human cerebral cortex (for reviews see Refs. 8–11). fNIRS enables investigation (without discomfort and interference related to the intrinsic limitations of PET and fMRI) of regional changes in oxyhemoglobin (O_2Hb) and deoxyhemoglobin (HHb) concentration in small vessels including capillary, arteriolar, and venular beds of the brain cortex.

The physiological significance of increased O_2Hb and decreased HHb on cortical activation has been extensively in-

vestigated in a rat brain model¹² and in humans.¹³ O_2Hb is the most sensitive indicator of changes in cerebral blood flow and the direction of the changes in HHb is determined by the degree of venous blood oxygenation and volume. In addition, studies combining either PET or fMRI with fNIRS have demonstrated that changes in oxygenation (reflecting the dynamic balance between oxygen supply and oxygen consumption), measured by fNIRS, correspond to signal intensity increases detected by fMRI (Refs. 14–16) and PET (Refs. 17 and 18).

To date, the most common approach of fNIRS is to measure light attenuation at two wavelengths between a pair of optical fibers set normal to the tissue surface at a known relative distance, to assume a fixed value of the scattering coefficient (μ'_s), and, by applying the Lambert-Beer law, to track the relative concentration changes in HHb and O_2Hb . This rather straightforward technique has been developed over time, resulting in instruments that operate at more wavelengths, with multiple-source and/or multiple-detector geometries. In particular, this latter feature offers the possibility to simultaneously probe different tissue regions to produce functional maps.

Address all correspondence to Valentina Quaresima, University of L'Aquila, Department of Biomedical Sciences and Technologies, 67100 L'Aquila, Italy. Tel: 39-0862-433516; Fax: 39-0862-433433; E-mail: vale@univaq.it

In the last 7 yr, multichannel fNIRS systems have been developed and tested to provide spatial maps¹⁹ (with a spatial resolution of about 0.5 cm) of changes in oxygenation in frontal, temporal, parietal, and visual cortical areas following different stimuli.^{20–24} In particular, the prefrontal cortex (the anterior portion of the frontal lobe) and the frontal lobe (the front part of the brain involved in planning, organizing, problem solving, selective attention, etc.), both involved in higher cognitive functions and in the determination of the personality, have been studied using various neuropsychological tests including mental calculation tasks, continuous performance task, Wisconsin Card Sorting task, color-word matching Stroop task, etc.^{25–44}

Another cognitive paradigm known to activate the prefrontal cortex is the verbal fluency task (VFT). The VFT is a neuropsychological task that enables assessment of the subject's ability to retrieve nouns based on a common criterion. The letter fluency version is based on a phonological criterion that requires the subject to pronounce as many words as possible beginning with a certain letter. Performances have been regarded to be mainly associated with frontal lobe function, particularly the left hemisphere.⁴⁵ During the execution of VFTs, maximum task-induced activation was observed in the left frontal regions, particularly in the left middle prefrontal gyrus and/or left inferior prefrontal gyrus using different methods including ¹³³Xe inhalation method,⁴⁶ fMRI (Ref. 47), PET (Ref. 48), and single-photon emission computed tomography⁴⁹ (SPECT). Some authors,^{50–53} using fMRI, have reported task-induced bilateral activation, particularly in the dorsolateral prefrontal and posterior parietal cortex.

To date, few fNIRS data about the prefrontal and frontal lobe involvement during VFT [using one/two-channel cw NIR (NIR_{cw}) systems] are available.^{26,30,36,43} The prefrontal cortex of both hemispheres was activated by the VFT, i.e., O₂Hb increased and HHb decreased significantly with respect to the corresponding baselines. Using multichannel fNIRS on both hemispheres, a significant increase in O₂Hb not accompanied by a decrease in HHb was found;⁴⁴ conversely, a significant increase in O₂Hb accompanied by a decrease in HHb was found in another study.³⁸

The results of these fNIRS studies confirm that the performance of the VFT leads to the activation in specific areas of the prefrontal cortex, without revealing a left lateralized activation. On the other hand, there is no strong evidence that cw fNIRS is sufficiently sensitive to reveal HHb changes, conventionally detected by fMRI.

The key limitations of the cw fNIRS technique are the coupling between the absorption and scattering coefficients (μ_a, μ_s') resulting in the lack of quantitative assessment, sensitivity to artifacts and experimental conditions. A possible way to uncouple μ_a from μ_s' is based on the use of sinusoidally modulated laser sources, and on the measurement of signal phase and amplitude changes induced by propagation. The frequency-domain (FD) technique extracts both the mean μ_s' and μ_a of the probed medium provided that a nontrivial calibration of collection efficiencies is performed. This approach has been successfully applied to measure tissue oxygenation, and has led to the first identification of a rapid change in μ_s' following a cerebral stimulus.⁵⁴ The dual approach is the study of photon migration in the time domain

and was first introduced *in vivo* by Chance et al.⁵⁵ and Delpy et al.⁵⁶ Furthermore, the temporal dispersion of a short laser pulse traveling through a diffusive medium can provide both the mean μ_s' and μ_a using a proper model of photon migration. In the past, the cost, size, and complexity of the time-resolved reflectance spectroscopy (TRS) instrumentation have prevented this technique from being effectively employed to study tissue oxygenation.

We have recently reported the development of a compact multichannel TRS tissue oximeter⁵⁷ (NIR_{TRS}). This system operates with two wavelengths, two injection points, and eight independent collection points, and has a typical acquisition time of 166 ms. Considering the controversial cw fNIRS results concerning the effects of the VFT on the prefrontal cortex, the aim of this study was to use our eight-channel NIR_{TRS} system to further investigate bilateral effects of the VFT-induced response within the prefrontal cortex.

2 Methods

2.1 System Setup

A compact two-source eight-channel NIR_{TRS} system was employed in this study. A pair of semiconductor pulsed lasers (PDL, Picoquant, Germany), working at 685 and 780 nm, with an 80-MHz repetition rate and a 1-mW average power, were used as light sources. Multimode graded-index fibers (50/125 μm) of different lengths and a fiber optics integrated device (VIS/NIR 2×2 fused splitter, OZ Optics, Canada) were used to multiplex in time the output pulses of the two laser heads so as to create two independent injection points. A compact 16-anode photomultiplier (R5900-01-L16, Hamamatsu, Japan) integrated with a 16-channel router (PML-16, Becker&Hickl, Germany) and a PC board (SPC-630, Becker&Hickl, Germany), for time-correlated single-photon counting (TCSPC), were used to detect and acquire time-resolved reflectance curves. Due to 20% optical crosstalk among adjacent channels, only 8 out of 16 channels were used by placing optical fiber on odd channels (1,3,5,...,15). In this configuration, the crosstalk was lower than 3%. The typical measurement time for the parallel acquisition of time-resolved curves from the 8 channels was 166 ms (6 Hz). A detailed description of the system is reported elsewhere.⁵⁷ In the most severe configuration for TCSPC, the maximum count rate should not exceed 8×10^5 photons/s (i.e., 0.01 photons detected per signal period with a 80-MHz repetition rate laser). Furthermore, the TCSPC board we employed in this study had 125-ns dead time (equivalent to a maximum acquisition frequency of 8 MHz) and a minimum acquisition time of 0.1 ms. Taking into account that the typical count rate from biological tissues is less than 10^6 photons/s, the combination of the lasers and the TCSPC board sets no practical limits to the detection of photons in TRS.

2.2 Data Analysis

Simultaneous estimation of μ_s' and μ_a can be achieved by best fitting time-resolved reflectance curves with a standard model of diffusion theory.⁵⁸ Therefore, to reduce dispersion of the fitted absorption coefficient values, we employed the modified Lambert-Beer law.⁵⁹ First, for each wavelength, a reference time-resolved reflectance curve $R_0(\rho, t, \lambda)$ was derived by averaging the curves corresponding to an initial rest-

ing period (typically 0.5 min). Fitting of $R_0(\rho, t, \lambda)$ yielded a reference absorption value $\mu_{a0}(\lambda)$, then $\Delta\mu_a(\lambda)$, the variation from the reference value, was derived according to

$$\mu_a(\lambda) = \mu_{a0}(\lambda) + \Delta\mu_a(\lambda), \quad (1)$$

$$\Delta\mu_a(\lambda) = -\frac{1}{vt} \ln \left[\frac{R(\rho, t, \lambda)}{R_0(\rho, t, \lambda)} \right]. \quad (2)$$

Improvement over the standard methods was more effective when the absorption was high. In this condition, standard fitting with the nonlinear least-squares methods yielded high dispersion in the fitted data.⁶⁰ A fitting range from 80% of the peak of TRS curve in the leading edge and 1% in the trailing edge of the TRS curve was chosen to estimate $\mu_{a0}(\lambda)$. For the estimation of $\Delta\mu_a(\lambda)$ from Eq. (2), the fitting range was 70 to 1% of both limits in the trailing edge, so as to enhance the contribution of late photons rather than early photons.

Assuming that O_2Hb and HHb are the major chromophores that contribute to tissue absorption, their respective concentrations are easily derived using the extinction coefficient.⁶¹ Indeed water absorption in this spectral region is much lower than hemoglobin absorption.⁶¹ A constant absorption (30%) was attributed to water and subtracted from μ_a prior to calculation of HHb and O_2Hb concentration. The total hemoglobin concentration ($tHb = O_2Hb + HHb$) and tissue oxygen saturation ($SO_2 = O_2Hb/tHb$, in percent) could then be derived.

During data analysis an integration time of 1 s was used to increase the SNR. This operation consisted in summing six time-resolved reflectance curves, each of which was acquired with a measurement time of 166 ms. After fitting the time-resolved reflectance curves, a 5-s average was applied to the data (i.e., data in Figs. 2 to 5 in Sec. 3 are represented with an effective sampling time of 5 s). Note that TCSPC uncertainty (i.e., the standard deviation over the average) in the estimation of μ_a is dramatically reduced when sampling time is augmented (either directly by incrementing the acquisition time, or indirectly by summing up several time-resolved reflectance curves acquired with a shorter acquisition time) since the total number of photons per curve is increased.

2.3 Subjects

Eight normal, right-handed, healthy volunteers (34.6 ± 8.7 yr) participated in this study. Informed consent was obtained from each subject after a full explanation of the nature of the procedure to be used and the noninvasiveness of the study. Throughout the study, subjects were lying on a comfortable bed in a quiet room. Right-handedness was evaluated by the Edinburgh Inventory of Handedness.⁶² Cardiac frequency was monitored by a pulse oximeter (N-200; Nellcor, Puritan Bennett, St. Louis, Missouri) with the sensor attached to the index finger of the right hand. The heart rate did not vary between the pretask and the task periods in all subjects (data not shown).

2.4 Verbal Fluency

A 2-min letter version of the VFT was adopted in this study.³⁰ Following a 2-min baseline (with eyes closed), subjects (preliminarily instructed properly) were asked to produce (overt

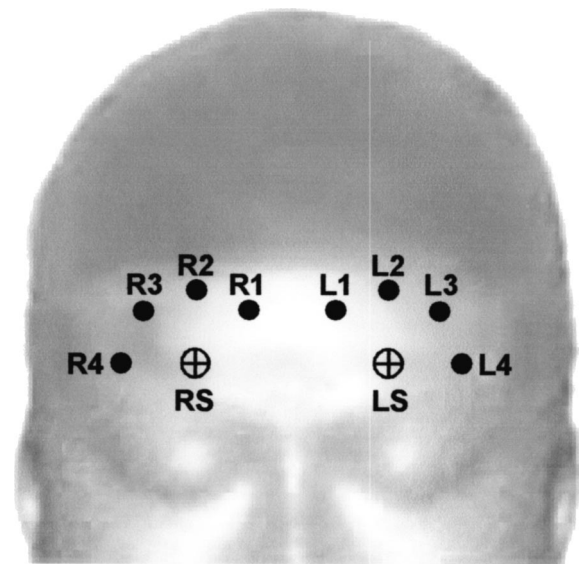


Fig. 1 Schematic representation of the optical probe and the eight measurement sites over the prefrontal lobe. The optical probes were centered at the Fp1 and Fp2 (according to the international 10–20 system for the EEG electrode placement) for the left (L) and right (R) sides (LS and RS), respectively. The source-detector distance was 3 cm.

speech) as many nouns as possible beginning with the letters “S,” “P,” “F,” and “C”. Each letter was acoustically presented every 30 s. No repetitions or proper nouns were permitted. Correct verbal responses were recorded for each subject. As a control task, subjects were requested to listen to a 2-min story.

The optical probe was placed over the head to cover the underlying prefrontal cortex and was centered (according to the international 10–20 system for the EEG electrode placement) at the Fp1 and Fp2 for left and right sides, respectively (Fig. 1). The frontal sinuses are located slightly below the lines between Fp1/Fp2. Only in some cases, the lines overlap the upper edge of the sinus. Therefore, the influence of the frontal sinuses on the NIRS measurements was considered negligible. The source-detector distance was 3 cm. No downward sliding of the fiber holders was observed at the end of the measurements in any subject.

Custom-made fibers holders were designed to keep fibers normally to the forehead by black plastic hollow tubes. Holders were kept in place on the head of the subject by biadhesive tape. The minimum distance between the light source located on the left (right) forehead and detectors placed over the right (left) forehead was 5 cm, to avoid crosstalk between optical signals detected simultaneously in the two areas.

2.5 Statistics

Changes (Δ) in SO_2 , tHb , O_2Hb , and HHb measured on the prefrontal cortex during the VFT were calculated by the difference between the rest condition (mean value over the 1.5- to 2-min baseline) and the end of the VFT (mean value over the last 30 s). The means and standard deviations of SO_2 , tHb , O_2Hb , and HHb values within left and right prefrontal cortex were determined separately and compared.

Statistics evaluation was carried out using the SPSS PC version 12.0 program (SPSS, Inc., Chicago, Illinois). Three-way repeated measures analysis of variance (RMANOVA) was applied to SO_2 , O_2Hb , HHb , and tHb as a dependent variable, with factors of side ($df=1$, left and right), measurement point ($df=7$), and condition ($df=1$). All three factors as well as two-way and three-way interactions among factors were included in the model.

When there was a significant main effect or interaction, we performed the RM ANOVA. Significant differences were identified using the Tukey's honestly significant difference multiple comparison test. The paired t test was used to compare the SO_2 , tHb , O_2Hb , and HHb values corresponding to each pair of left and right prefrontal cortex positions. The criterion for significance was $P<0.05$.

3 Results

The absolute values (average over the 1.5- to 2-min baseline) of SO_2 , O_2Hb , HHb , and tHb for each subject are reported in Table 1. The baseline values (grand average over the eight subjects) of O_2Hb , HHb , and tHb were homogeneous over the right prefrontal area. Some differences were found among the measurement points within the left hemisphere. Grand average SO_2 values of the most lateral measurement points (R4 and L4) were relatively lower than remaining ipsilateral values. Comparing paired measurements points (grand average values) in both hemispheres (R1 versus L1, R2 versus L2, etc.), no difference was found in O_2Hb , HHb , and tHb between left and right sides. Considering the grand average of SO_2 values, only L3 and L4 significantly differed from corresponding contralateral measurement points ($P=0.01$).

During the VFT, the subjects achieved a mean of 33.5 ± 10.3 number of correct responses for the four letters, showing similar performances in each of the four letter conditions ($S=7.9 \pm 2.4$, $P=8.6 \pm 3.3$, $F=8.6 \pm 2.6$, $C=8.4 \pm 2.6$).

The response in terms of prefrontal cortical oxygenation (measured as ΔO_2Hb , ΔHHb , and ΔtHb) to the VFT was variable amongst the subjects investigated. In particular, a typical prefrontal cortex activation response (measured indirectly by fNIRS) upon the VFT was³⁰ observed only in four (subjects: A, B, C, D) out of the seven subjects (one subject was excluded from the data analysis due to motion artifacts during the task). Figure 2 shows a single individual (subject A) as a representative of a typical prefrontal cortex ΔO_2Hb , ΔHHb , and ΔtHb response. In this subject, O_2Hb started to increase at the beginning of the VFT to reach a maximum change within the VFT, and it decreased progressively after the end of the task. Concomitantly, HHb decreased (not specularly) during the VFT, and it did not return to the pretask value within the observation time. The amplitude of the O_2Hb increase and HHb decrease was not uniform over the four measurement points within the right or the left side. The corresponding change in SO_2 is also reported in Fig. 2.

The larger increase of SO_2 and O_2Hb in the right compared to left hemisphere (Fig. 2) was no more evident when the response at each measurement site was averaged over the four subjects (A to D) (Fig. 3).

A significant VFT-mediated effect was found in SO_2 ($P<0.001$), HHb ($P<0.0001$), O_2Hb ($P<0.001$), and tHb ($P<0.05$) changes. A significant hemisphere-associated

effect was also observed in both SO_2 ($P<0.05$) and HHb ($P<0.01$), but not in O_2Hb and tHb changes. No significant influence of the measurement point factor on fNIRS parameters was found. In addition, no interaction was found between the three factors considered (task, hemispheres, and eight measurement points).

The time course of the grand average over the four subjects of each measured parameter (average of the responses over the four measurement points in the left or right side) is shown in Fig. 4.

The pattern of the O_2Hb , HHb , tHb , and SO_2 response to the VFT was variable among the three remaining subjects, with none comparable to that displayed in Figs. 2 and 3. In these subjects, an increase in SO_2 , O_2Hb , and tHb was observed during the task. Concomitantly, HHb decreased very rarely and, in most of the cases, did not change or increased at some measurement points. Furthermore, the O_2Hb , tHb , and SO_2 amplitude increase was not homogeneous over each side of the prefrontal cortex within the same subject. Figure 5 shows an individual (subject F) as a representative of an atypical ΔO_2Hb , ΔHHb , and ΔtHb response over the prefrontal area. Interestingly these three subjects (E, F, and G) had the same VFT performances as the others.

In all subjects, O_2Hb , HHb , tHb , and SO_2 tracings over the 2-min control task were not different from the corresponding baseline tracings.

4 Discussion

Verbal fluency tasks are designed to evaluate the spontaneous production of words beginning with a given letter (letter fluency; syntactic or phonetic association) or words beginning to a given class (category fluency; semantic association), within a limited amount of time.⁴⁵ These letter and category fluency paradigms (with a differential brain activation pattern) are frequently used in the assessment of patients with suspected prefrontal disorders. Deficits in word retrieval are probably the most serious impediment to effective communication in aphasics. Therefore, it is particularly important to identify which verbal fluency mechanisms can recover. Regional brain activity during phonological and semantic processing has been studied using fMRI, PET, SPECT, and transcranial Doppler sonography. During the execution of the VFT, maximum task-induced activation was observed in the left frontal regions particularly in the left middle prefrontal gyrus and/or left inferior prefrontal gyrus by different methods/techniques such as ^{133}Xe inhalation method,⁴⁶ fMRI (Ref. 47), PET (Ref. 48), and SPECT (Ref. 49). Some authors,⁵⁰⁻⁵³ using fMRI, have reported task-induced bilateral activation, particularly on the dorsolateral prefrontal and posterior parietal cortex. However, the category fluency task, and not the letter fluency task, has been reported to provoke a bilateral prefrontal activation response using⁶³ SPECT.

A recent study⁶⁴ evaluating whether VFT may specifically induce relatively greater left- than right-hemispheric activation in the dorsolateral prefrontal cortex has demonstrated that the desired effect could be achieved only in individuals with good performances on the VFT and not by poor performers who showed marked right-hemispheric activation. A significant bilateral blood flow velocity increase in the middle cerebral arteries was observed in response to 13 verbal and visu-

Table 1 Right (R) and left (L) prefrontal cortex SO_2 , tHb, HHb, and O_2Hb at the eight measurement points.

Subject	Parameter	R1	R2	R3	R4	L1	L2	L3	L4
A	$\text{SO}_2(\%)$	71.6(0.5)	73.9(0.5)	71.9(0.4)	69.4(0.5)	74.2(0.2)	73.0(0.3)	73.2(0.3)	72.7(0.4)
	tHb (μM)	80.3(0.8)	72.3(0.7)	55.6(0.4)	63.4(0.5)	69.3(0.3)	59.2(0.3)	51.2(0.3)	64.5(0.4)
	HHb (μM)	22.9(0.3)	18.8(0.2)	15.6(0.1)	19.4(0.2)	17.9(0.1)	16.0(0.2)	13.7(0.1)	17.6(0.2)
	O_2Hb (μM)	57.5(0.9)	53.4(0.9)	40.0(0.5)	44.0(0.6)	51.4(0.3)	43.2(0.4)	37.5(0.3)	46.9(0.5)
B	$\text{SO}_2(\%)$	73.7(0.3)	72.4(0.3)	68.0(0.5)	65.1(0.7)	75.6(0.3)	73.1(0.3)	74.3(0.3)	73.0(0.4)
	tHb (μM)	90.6(0.6)	86.4(0.6)	84.0(0.8)	82.6(0.9)	90.6(0.5)	83.1(0.4)	76.7(0.3)	82.7(0.5)
	HHb (μM)	23.8(0.2)	23.8(0.2)	26.9(0.3)	28.8(0.4)	22.1(0.2)	22.3(0.2)	19.7(0.2)	22.3(0.3)
	O_2Hb (μM)	66.8(0.6)	62.6(0.6)	57.2(0.8)	53.8(1.1)	68.5(0.6)	60.8(0.5)	56.9(0.4)	60.4(0.6)
C	$\text{SO}_2(\%)$	69.2(0.3)	69.8(0.5)	68.4(0.4)	69.0(0.6)	71.0(0.3)	69.1(0.3)	70.6(0.3)	69.7(0.5)
	tHb (μM)	85.0(0.5)	77.3(0.6)	72.7(0.5)	72.7(0.7)	83.5(0.3)	77.6(0.5)	73.1(0.3)	71.6(0.4)
	HHb (μM)	26.2(0.2)	23.4(0.3)	23.0(0.2)	22.5(0.3)	24.2(0.2)	24.0(0.2)	21.5(0.2)	21.7(0.3)
	O_2Hb (μM)	58.8(0.5)	53.9(0.8)	49.8(0.5)	50.2(0.8)	59.2(0.4)	53.7(0.5)	51.6(0.4)	49.9(0.6)
D	$\text{SO}_2(\%)$	67.5(0.6)	67.3(0.6)	63.5(0.5)	63.3(0.6)	68.7(0.3)	72.8(0.5)	69.4(1.0)	68.8(0.6)
	tHb (μM)	60.9(0.5)	67.6(0.6)	60.4(0.4)	64.5(0.6)	53.4(0.3)	62.9(0.4)	50.5(0.6)	53.8(0.4)
	HHb (μM)	19.8(0.3)	22.1(0.3)	22.1(0.3)	23.5(0.3)	16.7(0.1)	17.1(0.3)	15.4(0.4)	18.9(0.2)
	O_2Hb (μM)	41.1(0.7)	45.5(0.7)	38.4(0.5)	38.1(0.7)	36.7(0.3)	45.8(0.5)	35.0(0.8)	34.8(0.6)
E	$\text{SO}_2(\%)$	61.6(0.7)	71.1(0.7)	67.6(0.7)	63.4(0.8)	69.2(0.4)	69.8(0.6)	70.3(0.5)	66.6(0.6)
	tHb (μM)	55.2(0.7)	60.3(1.0)	53.0(0.7)	58.1(0.9)	64.6(0.8)	61.7(1.0)	58.2(0.7)	65.7(1.3)
	HHb (μM)	21.2(0.3)	17.4(0.3)	17.2(0.3)	21.3(0.4)	19.9(0.2)	18.6(0.2)	17.3(0.2)	21.9(0.3)
	O_2Hb (μM)	34.0(0.7)	42.9(1.0)	35.8(0.8)	36.9(1.0)	44.8(0.8)	43.1(1.0)	40.9(0.8)	43.8(1.2)
F	$\text{SO}_2(\%)$	72.0(0.3)	74.9(0.4)	75.3(0.4)	76.0(0.4)	79.1(0.3)	77.4(0.4)	76.4(0.3)	76.6(0.4)
	tHb (μM)	44.0(0.3)	63.4(0.6)	65.2(0.7)	69.5(0.6)	58.6(0.4)	70.3(0.4)	63.1(0.3)	72.3(0.5)
	HHb (μM)	12.3(0.1)	15.9(0.1)	16.1(0.2)	16.7(0.2)	12.2(0.1)	15.9(0.2)	14.9(0.1)	16.9(0.2)
	O_2Hb (μM)	31.7(0.4)	47.5(0.6)	49.1(0.8)	52.8(0.7)	46.4(0.5)	54.4(0.6)	48.2(0.3)	55.4(0.6)
G	$\text{SO}_2(\%)$	68.7(0.4)	69.2(0.4)	67.4(0.4)	62.5(0.5)	68.5(0.4)	67.4(0.5)	68.5(0.5)	66.4(0.4)
	tHb (μM)	77.4(0.5)	76.5(0.5)	73.1(0.4)	76.7(0.6)	81.1(0.4)	78.6(0.6)	77.8(0.4)	83.8(0.5)
	HHb (μM)	24.2(0.2)	23.6(0.2)	23.8(0.2)	28.7(0.2)	25.6(0.3)	25.6(0.3)	24.5(0.3)	28.1(0.3)
	O_2Hb (μM)	53.2(0.6)	53.0(0.6)	49.3(0.5)	47.9(0.7)	55.5(0.5)	53.0(0.7)	53.3(0.6)	55.7(0.6)

ospatial tasks by using transcranial Doppler sonography.⁶⁵ Five verbal tasks showed a significant left-hemispheric lateralization that can best be elicited by linguistic tasks that require active or creative processing of the verbal material such as constructing a sentence with given words or retrieving words. The bilateral increase of blood flow velocity in the middle cerebral arteries on VFT is consistent with the increase of O_2Hb observed during VFT in this study by NIR_{TRS} and in other studies using a one-/two-channel NIR_{CW} systems^{26,30,36,43}

and by multichannel NIR_{CW} systems.^{38,44} Although the increase of O_2Hb on VFT is usually accompanied by a smaller decrease in HHb, in our study, this pattern was not observed in three out of the seven subjects. For this reason the oxygenation response to VFT was averaged over four subjects only (Figs. 3 and 4). However, the letter version of the VFT adopted in our study and the recorded number of correct verbal responses were comparable to those reported in a recent study.³⁰

Table 1 (Continued.)

Subject	Parameter	R1	R2	R3	R4	L1	L2	L3	L4
H	SO ₂ (%)	66.9(0.4)	69.2(0.3)	67.1(0.4)	64.9(0.6)	65.9(0.3)	68.0(0.4)	67.6(0.3)	65.0(0.4)
	tHb (μM)	70.1(0.5)	67.0(0.4)	69.4(0.5)	72.8(0.8)	75.1(0.5)	68.9(0.5)	68.2(0.4)	71.8(0.4)
	HHb (μM)	23.2(0.2)	20.6(0.2)	22.8(0.2)	25.6(0.3)	25.6(0.2)	22.0(0.2)	22.1(0.2)	25.2(0.2)
	O ₂ Hb (μM)	46.9(0.6)	46.4(0.5)	46.6(0.6)	47.2(0.9)	49.4(0.5)	46.9(0.6)	46.1(0.4)	46.6(0.5)
Grand average	SO ₂ (%)	68.9±3.8	71.0±2.6	68.7±3.5	66.7±4.6*	71.5±4.4	71.3±3.4	71.3±3.1^	69.9±4.0^
	tHb (μM)	70.4±16.0	71.4±8.5	66.7±10.3	70.0±7.9	72.0±12.9	70.3±8.8	64.9±10.9°	70.8±9.8
	HHb (μM)	21.7±4.3	20.7±3.0	20.9±4.1	23.3±4.3	20.5±4.8	20.2±3.8	18.6±3.9°	21.6±3.8
	O ₂ Hb (μM)	48.8±12.5	50.7±6.3	45.7±7.2	46.4±6.3	51.5±9.7	50.1±6.3	46.2±7.8°	49.2±8.1

The site number referred to is in Fig. 1.

The numbers in parenthesis represent the SD of the mean values of each fNIRS parameter over the corresponding 1.5- to 2-min baseline.

Grand average data are presented as means±SD.

N=8.

*Significantly different from R2 (P<0.01).

°Significantly different from L1 (P<0.05).

^Significantly different from the corresponding contralateral one (P=0.01).

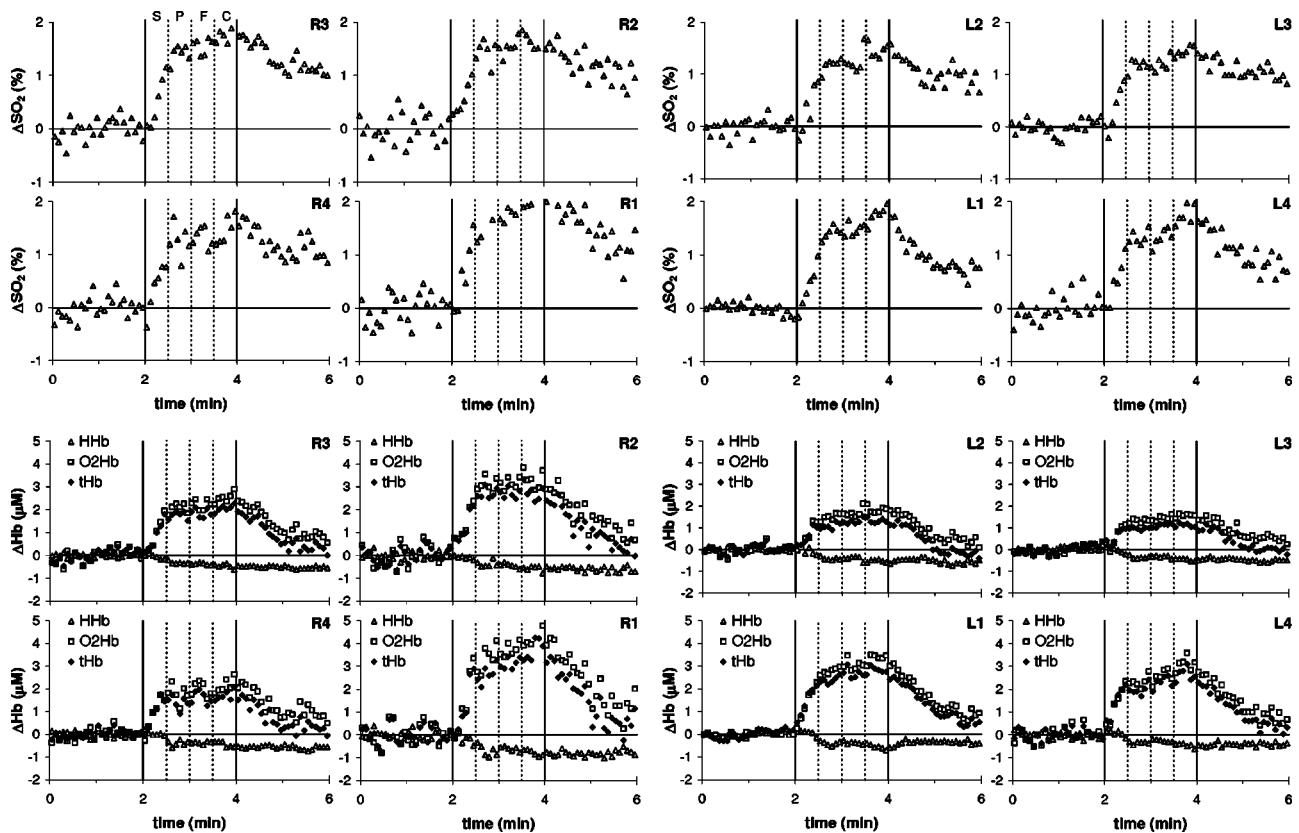


Fig. 2 Typical topographic presentation of the time courses of ΔSO_2 , $\Delta\text{O}_2\text{Hb}$, ΔHHb , and ΔtHb on VFT over eight measurement sites on the right (R) and left (L) prefrontal cortex (subject A). Arrangement of results resembles the measurement positions in Fig. 1. Continuous vertical lines indicate total duration of the VFT, which is in turn subdivided by the three dotted vertical lines in four intervals. Each interval represents the allocated time for each subject to produce as many nouns as possible beginning with the corresponding reported letter (upper left panel).

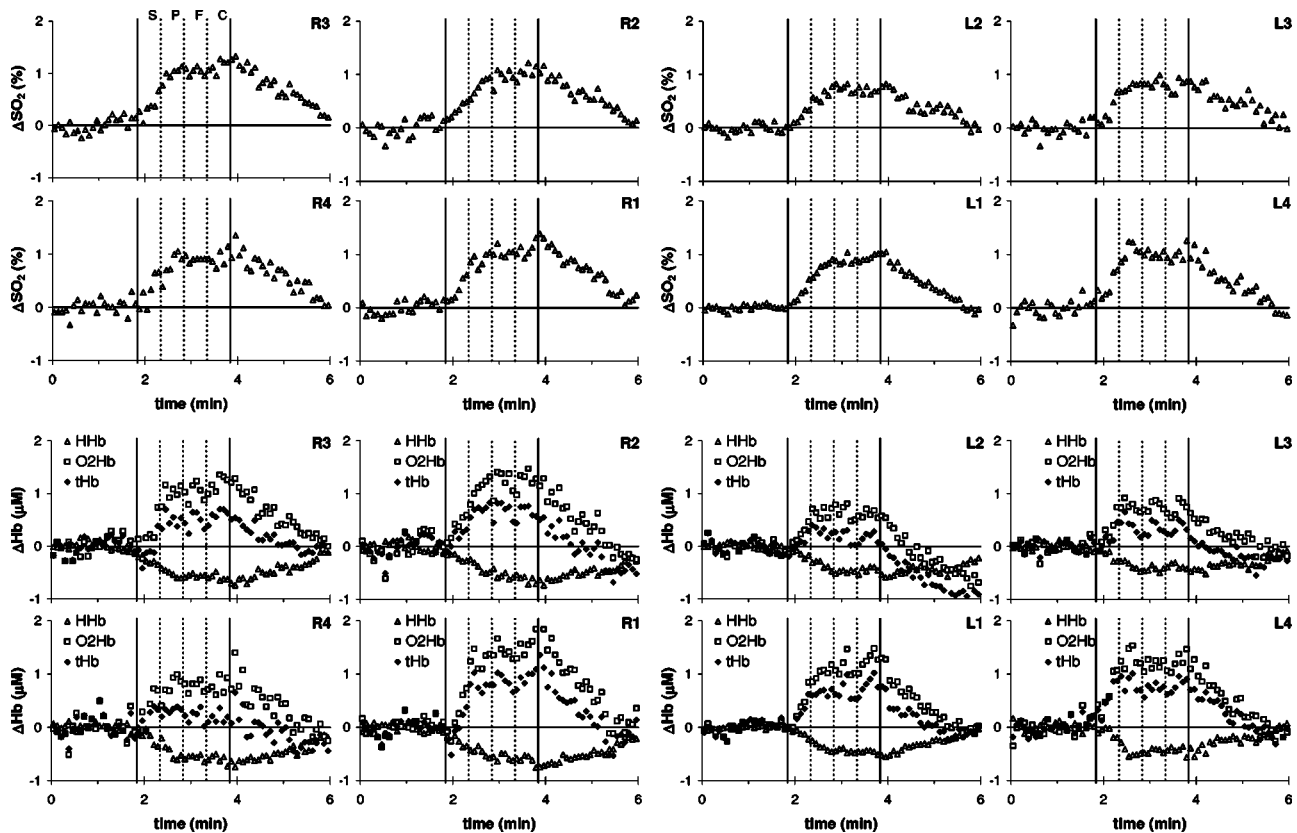


Fig. 3 Topographic presentation of the time courses of ΔSO_2 , $\Delta\text{O}_2\text{Hb}$, ΔHHb , and ΔtHb on VFT over eight measurement sites on the right (R) and left (L) prefrontal cortex. Arrangement of results resembles measurement positions in Fig. 1, expressed as the average over four subjects. Continuous vertical lines indicate total duration of the VFT, which is in turn subdivided by the three dotted vertical lines in four intervals. Each interval represents the allocated time for each subject to produce as many nouns as possible beginning with the corresponding reported letter (upper left panel).

With respect to the amplitude of the cortical activation response between hemispheres, taking into account intersubjects variability, only SO_2 increase during VFT was significantly higher in right ($1.1 \pm 0.5\%$) compared to left prefrontal cortex ($0.9 \pm 0.5\%$) ($P = 0.005$). The VFT-related change in the remaining measured parameters (O_2Hb , HHb , and tHb , as reported by other groups^{30,38}) is superimposable over both left and right sides of the prefrontal cortex (Fig. 4). Our results confirm that, in some cases, the oxygenation response to the VFT is bilateral and symmetrical. Recently, hemodynamic differences in the activation of the prefrontal cortex during VFT and attention tasks (letter cancellation and continuous performance test) have been investigated using⁴³ a two-channel NIRS. While O_2Hb bilaterally increased with a concurrent decrease in HHb during the VFT, both O_2Hb and HHb bilaterally increased during the activation due to the task of attention. It was suggested that HHb measurement may therefore provide an objective index of the subjective effort to pay attention. The impairment of prefrontal lobe functions has been repeatedly documented in major psychiatric disorders, with O_2Hb increases during VFT significantly lower in association with major depressive disorders and bipolar disorders.³⁶ This result is not explained by differences of performance, since no difference in the number of words answered was found among these three groups. In addition, no significant difference of HHb response was found.³⁶

The different cortical activation pattern observed in three out of the seven subjects, characterized by a lack of HHb decrease or even an HHb increase during the VFT (Fig. 5) may be partly explained by the involvement of additional mechanisms (i.e., of attention, association, etc.) besides the specific ones for the letter fluency task. In this manner, other cortical areas (not under investigation) could have been concomitantly activated and/or the oxygen consumption in the investigated area could have been higher⁴³ than that one observed in the subjects with an activation response characterized by a marked increase in O_2Hb and tHb , and a decrease in HHb . This latter cortical response (found in four out of the seven subjects), defined as the typical one, is interpreted as a mismatch between a major increase in the regional cerebral blood flow (and blood volume) and a minor increase in oxygen consumption over the activated cortical area.⁶⁶ On the other hand, the constant level of HHb (found in most measurement points of three out of the seven subjects) could have resulted from an increase in the regional cerebral metabolic rate for oxygen, compensated by an increase in the regional cerebral blood flow. Therefore, the increase in HHb (found in some measurement points of three out of the seven subjects) may result from a further increase in oxygen consumption with a consequent mismatch between blood flow increase and oxygen consumption increase this time in favor of the latter one.

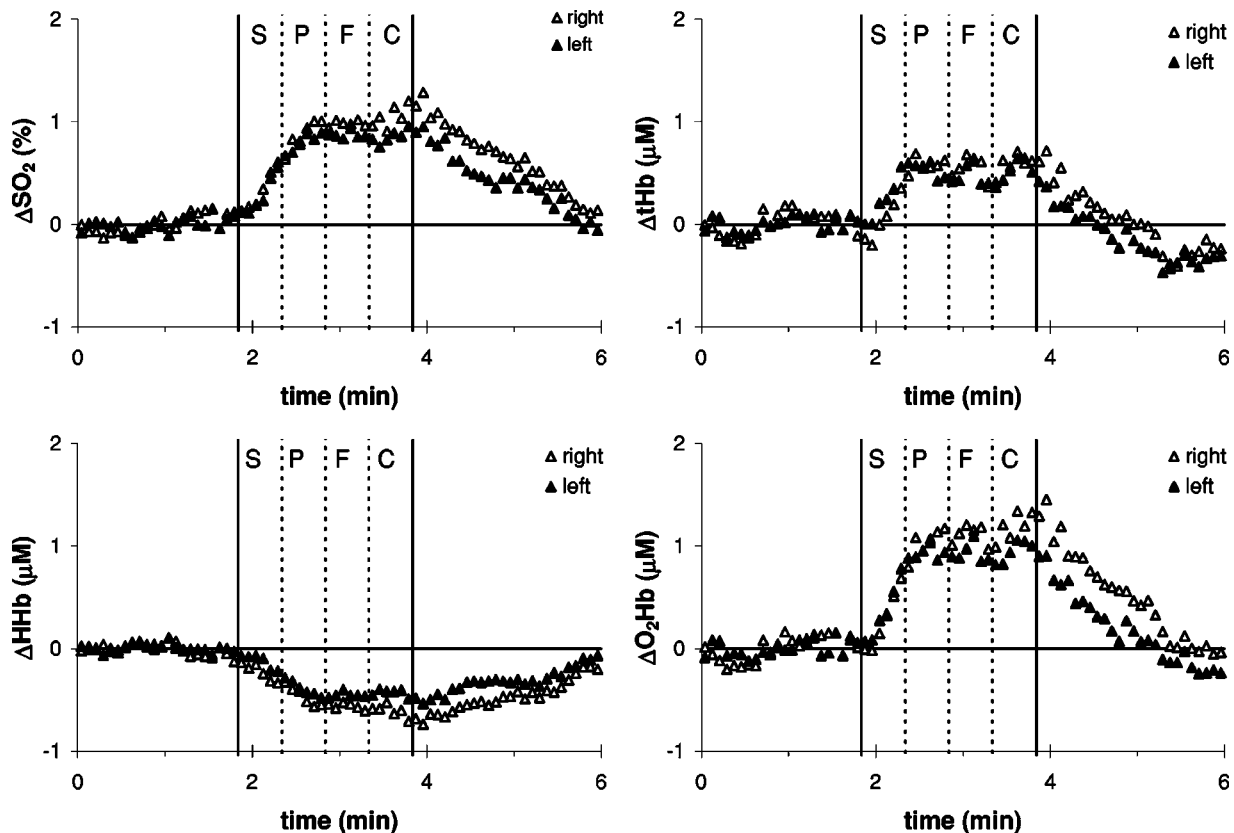


Fig. 4 Grand average over the four subjects of the time course of ΔSO_2 , $\Delta\text{O}_2\text{Hb}$, ΔHHb , and ΔtHb on the VFT. For each subject, the response of each parameter to VFT is reported as the mean of the responses of four measurement points on the right or the left prefrontal cortex. Continuous vertical lines indicate total duration of the VFT, which is in turn subdivided by the three dotted vertical lines in four intervals. Each interval represents the allocated time for each subject to produce as many nouns as possible beginning with the corresponding reported letter (upper left panel).

The lack of HHb decrease may be also explained by the decrease in blood flow velocity probably due to the increased resistance of the capillary venous wind kessel. Indeed, HHb is washed out of the activated cortical area faster than it is generated (typical response), as demonstrated by the increase in blood flow velocity.⁶⁵ Another possible reason of a lack of HHb decrease could be the diverse neuroanatomy of the three subjects with respect to the others. Since, in this study the fNIRS measurements were not combined with those from MRI or computed tomography (CT), and/or fMRI, PET, transcranial Doppler sonography, and angiography, it is difficult to provide a concrete interpretation of HHb behavior in the three anomalous subjects (E, F, and G).

In this study, no significant heart rate changes were found during the VFT. Therefore, during the VFT, SO_2 , O_2Hb , and HHb changes observed at each measurement point were task-related responses and not the consequence of a generalized increase in cerebral blood flow, as would be expected in the case of an increased heart rate.²²

A brief summary of current NIRS instrumentation for muscle and brain studies can be found elsewhere.⁵⁷ A detailed review on technological advantages/disadvantages of cw, FD, and TRS instrumentation in fNIRS studies has been reported previously.¹¹ Here, we focus on the advantages and/or disadvantages of using fNIRS in cognitive studies over other functional imaging techniques. First, it is possible to indepen-

dently quantitate temporal changes in O_2Hb , HHb, and tHb. Furthermore, if TRS or FD are employed, SO_2 can also be estimated, providing a further indicator of brain activation. Second, there is no noise associated with fNIRS measurement techniques, whereas noise associated with fMRI could interfere with auditory stimuli and subject attention levels. Third, a high SNR enables the observation of changes in oxygenation even in response to a single trial, as previously shown.⁶⁷ Fourth, fNIRS has fewer artifacts due to head motion than fMRI. Fifth, fNIRS makes it possible to detect overt verbal responses that may provoke artifacts in fMRI. Sixth, fNIRS has a high temporal resolution together with the unique advantage of being compact and transportable, enabling measurements in a natural environment. Conditions under which tests are performed using fMRI or PET do not fit classical neuropsychological test conditions, i.e., sitting at a table or in front of a computer screen in a quiet room.

On the other hand, fNIRS measurements are restricted mainly to the cortical surface, the spatial accuracy during focal hemodynamic changes is limited due to the effect of light diffusion and the contribution of extracranial artifacts should be carefully evaluated.⁶⁸ A recent study, performed on 17 subjects, has demonstrated that in Fp1 the depth of the cortical surface from the skin is⁶⁹ 13.5 ± 2.2 mm. This means that the optical path length differs among individuals by about 5 mm.

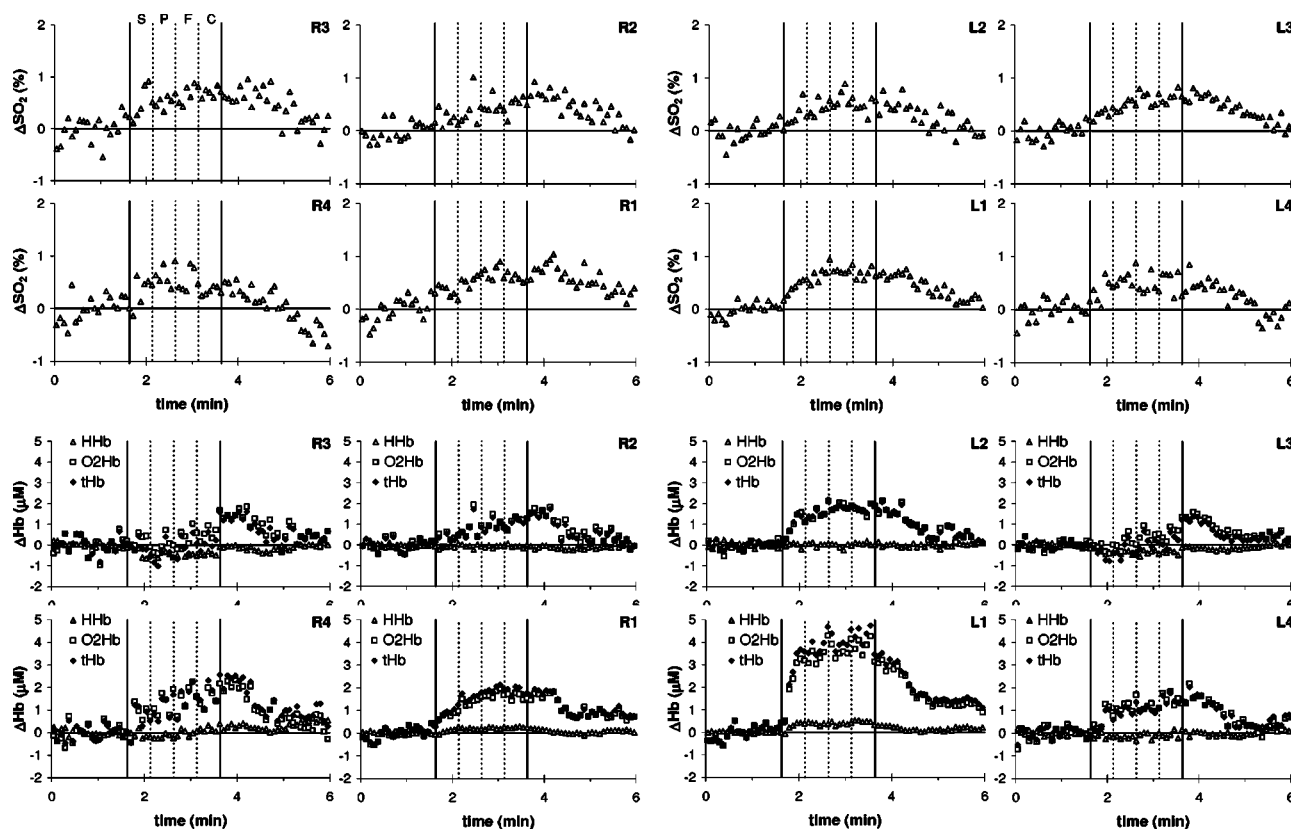


Fig. 5 Topographic presentation of the time courses of ΔSO_2 , $\Delta\text{O}_2\text{Hb}$, ΔHHb , and ΔtHb on VFT over eight measurement sites on the right (R) and left (L) prefrontal cortex (subject F). Arrangement of results resembles measurement positions in Fig. 1. Continuous vertical lines indicate total duration of the VFT, which is in turn subdivided by the three dotted vertical lines in four intervals. Each interval represents the allocated time for each subject to produce as many nouns as possible beginning with the corresponding reported letter (upper left panel).

Different cortical depths among channels can cause a similar problem of varying optical path lengths when a large area is measured by multichannel NIRS. The problems of spatial accuracy, signal contamination by superficial fluctuations, and spatial nonhomogeneity of head tissues could be resolved using multiple source-detector probes and applying new methods of 3-D reconstruction currently under development.^{13,24,70} The sensitivity of the NIRS signal to cortical activity changes depends on both the depth of the inner skull and the thickness of the cerebrospinal fluid, as well as the partial path length in the brain and, hence, cannot be predicted from the depth of the brain surface alone.^{68,69} Differences in optical path length cause⁷¹ crosstalk between O_2Hb and HHb . As previously suggested, an image reconstruction algorithm that predicts the path length in the activated region of the brain might reduce the crosstalk in the measurement more effectively than a calculation using the mean optical path length.¹³

NIR_{TRS} estimates absolute concentration values (averaged over the investigated tissue volume) of O_2Hb and HHb , from which tHb can be derived. The possibility to map tHb , which strictly relates to tissue blood volume, over a large cortical area may enable regional evaluation of vasodilatation and/or capillary recruitment. Furthermore, by measuring O_2Hb and HHb , NIR_{TRS} enables the quantification of SO_2 in the tissue blood volume considered. Cerebral cortex SO_2 predominantly reflects saturation of the intracranial venous compartment of circulation.⁷² SO_2 measurements are extremely important in

clinics suggesting potential use of NIR_{TRS} instruments for cortical SO_2 mapping (i.e., to evaluate the cerebrovascular reactivity in the neurovascular diseases and/or to evaluate the efficacy of stroke therapy/rehabilitation). For example, a difference between asymptomatic and symptomatic patients suffering from carotid occlusive disease has been recently demonstrated (in terms of SO_2 increase) using a FD oximeter during a CO_2 reactivity test.⁷³ For medical applications, the normal range of tHb and SO_2 in the brain must be studied in a large population to determine normal and abnormal value ranges. The cross-subject mean SO_2 values in our study (Table 1) were $68.8 \pm 3.2\%$ (right) and $71.0 \pm 3.6\%$ (left) and are similar to those reported using a FD oximeter.^{73,74} The cross-subject average tHb values (Table 1) were $69.6 \pm 9.6 \mu\text{M}$ (right) and $69.5 \pm 9.9 \mu\text{M}$ (left) and are also similar to those obtained using a FD oximeter.⁷⁴

It is foreseen that the NIR_{TRS} system may have advantages over NIR_{CW} systems, especially in terms of increased penetration depth. In particular, in contrast to CW systems, in which sensitivity to depth is obtained by increasing the distance between source and detector, the TRS system sensitivity to depth can be obtained at a fixed source detector distance by selecting late photons.^{75,76} However, to exploit information encoded in the late photons, it is necessary to make several *a priori* assumptions on the structure of the head (typically modeled as a layered medium consisting of scalp, skull, cere-

brospinal fluid, and brain) and on its optical properties.⁷⁶ Currently, however, there is little knowledge of the *in vivo* optical properties of brain tissues, making the interpretation of experimental data difficult in terms of a layered model. Here, we used a homogeneous model for photon diffusion to estimate changes in μ_a as for standard approaches used by cw instrumentation (Hamamatsu NIRO-300, Hitachi ETG-100, etc). Yet, as described in the Sec. 2, we derived $\Delta\mu_a$ by using photons in the tail of the TRS curve that have therefore probed deeper structures, when compared to cw measurements performed at the same source-detector distance.

5 Conclusion

The mapping of brain functions by fNIRS is today no longer a challenge, with promising results obtained using simple cw instruments and more recently even FD systems have been successfully employed. In this paper, we reported the use of a TRS system to monitor brain hemodynamic responses to a cognitive paradigm. For the first time, to our knowledge, we reported the possibility to map SO_2 as well as O_2Hb , HHb , and tHb simultaneously and bilaterally over a large area of the prefrontal cortex at “rest” and during cognitive stimuli, such as the VFT. Furthermore, we reported (in four out of the seven subjects) that after the beginning of the VFT a bilateral O_2Hb increase is accompanied by a HHb decrease. Our results are in agreement with similar experiments performed using cw fNIRS and fMRI, demonstrating the potentiality of a TRS approach. Although the correlation between variables of different neuroimaging techniques must be further elucidated, the clear activation in right and left hemispheres upon a verbal task (such as encoding words) suggests that fNIRS may be better at detecting cerebral activation than other conventional neuroimaging techniques. Finally, considering the necessity to map broader brain areas to better investigate the relationship between different brain regions, work is in progress to improve our instrument replacing the fused splitter with a fiber optics switch, to further increase the number of injection points from two to nine, and reduce the acquisition times to 100 ms. Also, by means of a newly developed photomultiplier tube, it is foreseen to double the number of independent collection channels.

Acknowledgments

This work is partially supported by MEDPHOT Thematic Network (EC QLG1-CT-2000-01464) and by COFIN2000 (MM02163721).

References

1. F. F. Jobsis-VanderVliet, “Discovery of the near-infrared window into the body and the early development of near-infrared spectroscopy,” *J. Biomed. Opt.* **4**, 392–396 (1999).
2. D. T. Delpy and M. Cope, “Quantitation in tissue near-infrared spectroscopy,” *Phil. Trans. R. Soc. Lond. Biol. Sci.* **261**, 649–659 (1997).
3. P. L. Madsen and H. N. Secher, “Near-infrared oximetry of the brain,” *Prog. Neurobiol.* **58**, 541–560 (1999).
4. K. K. McCully and T. Hamaoka, “Near-infrared spectroscopy: what can it tell us about oxygen saturation in skeletal muscle?” *Exercise Sport Sci. Rev.* **28**, 123–127 (2000).
5. A. Villringer, J. Planck, C. Hock, L. Schleichkofer, and U. Dirnagl, “Near infrared spectroscopy (NIRS): a new tool to study hemodynamic changes during activation of brain function in human adults,” *Neurosci. Lett.* **154**, 101–104 (1993).
6. A. Chance, Z. Zhuang, C. UnAh, C. Alter, and L. Lipton,

- “Cognition-activated low-frequency modulation of light absorption in human brain,” *Proc. Natl. Acad. Sci. U.S.A.* **90**, 3770–3774 (1993).
7. Y. Hoshi and M. Tamura, “Dynamic multichannel near-infrared optical imaging of human brain activity,” *J. Appl. Physiol.* **75**, 1842–1846 (1993).
8. G. Gratton, M. Fabiani, T. Elbert, and B. Rockstroh, “Seeing right through you: applications of optical imaging to the study of the human brain,” *Psychophysiology* **40**, 487–491 (2003).
9. Y. Hoshi, “Functional near-infrared optical imaging: utility and limitations in human brain mapping,” *Psychophysiology* **40**, 511–520 (2003).
10. H. Obrig and A. Villringer, “Beyond the visible-imaging the human brain with light,” *J. Cereb. Blood Flow Metab.* **23**, 1–18 (2003).
11. G. Strangman, D. A. Boas, and J. P. Sutton, “Non-invasive neuroimaging using near-infrared light,” *Biol. Psychiatry* **52**, 679–693 (2002).
12. Y. Hoshi, N. Kobayashi, and M. Tamura, “Interpretation of near-infrared spectroscopy signals: a study with a newly developed perfused rat brain model,” *J. Appl. Physiol.* **90**, 1657–1662 (2001).
13. D. A. Boas, T. Gaudette, G. Strangman, X. Cheng, J. J. Marota, and J. B. Mandeville, “The accuracy of near infrared spectroscopy and imaging during focal changes in cerebral hemodynamics,” *Neuroimage* **13**, 76–90 (2001).
14. D. J. Mehagnoul-Schippier, B. F. van der Kallen, W. N. Colier, M. C. van der Sluijs, L. J. van Erning, H. O. Thijssen, B. Oeseburg, W. H. Hoefnagels, and R. W. Jansen, “Simultaneous measurements of cerebral oxygenation changes during brain activation by near-infrared spectroscopy and functional magnetic resonance imaging in healthy young and elderly subjects,” *Hum. Brain Mapp* **16**, 14–23 (2002).
15. G. Strangman, J. P. Culver, J. H. Thompson, and D. A. Boas, “A quantitative comparison of simultaneous BOLD fMRI and NIRS recordings during functional brain activation,” *Neuroimage* **17**, 719–773 (2002).
16. V. Toronov, A. Webb, J. H. Choi, M. Wolf, A. Michalos, E. Gratton, and D. Hueber, “Investigation of human brain hemodynamics by simultaneous near-infrared spectroscopy and functional magnetic resonance imaging,” *Med. Phys.* **28**, 521–527 (2001).
17. C. Hock, K. Villringer, F. Muller-Spahn, R. Wenzel, H. Heekeren, S. Schuh-Hofer, M. Hofmann, S. Minoshima, M. Schwaiger, U. Dirnagl, and A. Villringer, “Decrease in parietal cerebral hemoglobin oxygenation during performance of a verbal fluency task in patients with Alzheimer’s disease monitored by means of near-infrared spectroscopy (NIRS)-correlation with simultaneous rCBF-PET measurements,” *Brain Res.* **755**, 293–303 (1997).
18. E. Rostrup, I. Law, F. Pott, K. Ide, and G. M. Knudsen, “Cerebral hemodynamics measured with simultaneous PET and near-infrared spectroscopy in humans,” *Brain Res.* **954**, 183–193 (2002).
19. J. C. Hebden, “Advances in optical imaging of the newborn infant brain,” *Psychophysiology* **40**, 501–510 (2003).
20. W. N. Colier, V. Quaresima, R. Wenzel, M. C. van der Sluijs, B. Oeseburg, M. Ferrari, and A. Villringer, “Simultaneous near-infrared spectroscopy monitoring of left and right occipital areas reveals contra-lateral hemodynamic changes upon hemi-field paradigm,” *Vision Res.* **4**, 97–102 (2001).
21. M. A. Franceschini, S. Fantini, J. H. Thompson, J. P. Culver, and D. A. Boas, “Hemodynamic evoked response of the sensorimotor cortex measured noninvasively with near-infrared optical imaging,” *Psychophysiology* **40**, 548–560 (2003).
22. M. A. Franceschini, V. Toronov, M. E. Filiaci, E. Gratton, and S. Fantini, “On-line optical imaging of the human brain with 160-ms temporal resolution,” *Opt. Express* **6**, 49–57 (2000).
23. G. Jaszewski, G. Strangman, J. Wagner, K. K. Kwong, R. A. Poldrack, and D. A. Boas, “Differences in the hemodynamic response to event-related motor and visual paradigms as measured by near-infrared spectroscopy,” *Neuroimage* **20**, 479–488 (2003).
24. H. Koizumi, T. Yamamoto, A. Maki, Y. Yamashita, H. Sato, H. Kawaguchi, and N. Ichikawa, “Optical topography: practical problems and new applications,” *Appl. Opt.* **42**, 3054–3062 (2003).
25. A. A. Baird, J. Kagan, T. Gaudette, K. A. Walz, N. Hershlag, and D. A. Boas, “Frontal lobe activation during object permanence: data from near-infrared spectroscopy,” *Neuroimage* **16**, 1120–1125 (2002).
26. A. J. Fallgatter, M. Roesler, L. Sitzmann, A. Heidrich, T. J. Mueller, and W. K. Strik, “Loss of functional hemispheric asymmetry in

- Alzheimer's dementia assessed with near-infrared spectroscopy," *Brain Res. Cogn. Brain Res.* **6**, 67–72 (1997).
27. J. Fallgatter and W. K. Strik, "Frontal brain activation during the Wisconsin Card Sorting Test assessed with two-channel near-infrared spectroscopy," *Eur. Arch. Psychiatry Clin. Neurosci.* **248**, 245–249 (1998).
 28. J. Fallgatter and W. K. Strik, "Reduced frontal functional asymmetry in schizophrenia during a cued continuous performance test assessed with near-infrared spectroscopy," *Schizophr. Bull.* **26**, 913–919 (2000).
 29. M. J. Herrmann, A. C. Ehlis, and A. J. Fallgatter, "Prefrontal activation through task requirements of emotional induction measured with NIRS," *Biol. Psychol.* **64**, 255–263 (2003).
 30. M. J. Herrmann, A. Ehlis, and A. J. Fallgatter, "Frontal activation during a verbal-fluency task as measured by near infrared spectroscopy," *Brain Res. Bull.* **61**, 51–56 (2003).
 31. Y. Hoshi, I. Oda, Y. Wada, Y. Ito, Y. Yamashita, M. Oda, K. Ohta, Y. Yamada, and M. Tamura, "Visuospatial imagery is a fruitful strategy for the digit span backward task: a study with near-infrared optical tomography," *Brain Res. Cogn. Brain Res.* **9**, 339–342 (2000).
 32. Y. Hoshi, B. H. Tsou, V. A. Billock, M. Tanosaki, Y. Iguchi, M. Shimada, T. Shinba, Y. Yamada, and I. Oda, "Spatiotemporal characteristics of hemodynamic changes in the human lateral prefrontal cortex during working memory tasks," *Neuroimage* **20**, 1493–1504 (2003).
 33. Y. Hoshi and S. J. Chen, "Regional cerebral blood flow changes associated with emotions in children," *Pediatr. Neurol.* **27**, 275–281 (2002).
 34. R. P. Kennan, D. Kim, A. Maki, H. Koizumi, and R. T. Constable, "Non-invasive assessment of language lateralization by transcranial near infrared optical topography and functional MRI," *Hum. Brain Mapp* **16**, 183–189 (2002).
 35. K. Matsuo, T. Kato, M. Fukuda, and N. Kato, "Alteration of hemoglobin oxygenation in the frontal region in elderly depressed patients as measured by near-infrared spectroscopy," *J. Neuropsychiatry Clin. Neurosci.* **12**, 465–471 (2000).
 36. K. Matsuo, N. Kato, and T. Kato, "Decreased haemodynamic response to cognitive and physiological tasks in mood disorders as shown by near-infrared spectroscopy," *Psychol. Med.* **32**, 1029–1037 (2002).
 37. K. Matsuo, T. Kato, K. Taneichi, A. Matsumoto, T. Ohtani, T. Hamamoto, H. Yamasue, Y. Sakano, T. Sasaki, M. Sadamatsu, A. Iwanami, N. Asukai, and N. Kato, "Activation of the prefrontal cortex to trauma-related stimuli measured by near-infrared spectroscopy in posttraumatic stress disorder due to terrorism," *Psychophysiology* **40**, 492–500 (2003).
 38. K. Matsuo, K. Taneichi, A. Matsumoto, T. Ohtani, H. Yamasue, Y. Sakano, T. Sasaki, M. Sadamatsu, K. Kasai, A. Iwanami, N. Asukai, N. Kato, and T. Kato, "Hypoactivation of the prefrontal cortex during verbal fluency test in PTSD: a near-infrared spectroscopy study," *Psychiatry Res.: Neuroimag.* **124**, 1–10 (2003).
 39. V. Quaresima, M. Ferrari, M. C. van der Sluijs, J. Menssen, and W. N. Colier, "Lateral frontal cortex oxygenation changes during translation and language switching revealed by non-invasive near-infrared multi-point measurements," *Brain Res. Bull.* **59**, 235–243 (2002).
 40. M. Peña, A. Maki, D. Kovacic, G. Dehaene-Lambertz, H. Koizumi, F. Bouquet, and J. Mehler, "Sounds and silence: optical topography study of language recognition at birth," *Proc. Natl. Acad. Sci. U.S.A.* **100**, 11702–11705 (2003).
 41. M. L. Schroeter, S. Zysset, T. Kupka, F. Kruggel, and D. Y. von Cramon, "Near-infrared spectroscopy can detect brain activity during a color-word matching Stroop task in an event-related design," *Hum. Brain Mapp* **17**, 61–71 (2002).
 42. T. Shimba, M. Nagano, N. Kariya, K. Ogawa, T. Shinozaki, S. Shimamoto, and Y. Hoshi, "Near-infrared spectroscopy analysis of frontal lobe dysfunction in schizophrenia," *Biol. Psychiatry* **20**, 1–13 (2003).
 43. M. Toichi, R. L. Findling, Y. Kubota, J. R. Calabrese, M. Wiznitzer, N. K. McNamara, and K. Yamamoto, "Hemodynamic differences in the activation of the prefrontal cortex: attention vs. higher cognitive processing," *Neuropsychologia* **42**, 698–706 (2004).
 44. A. Watanabe, K. Matsuo, N. Kato, and T. Kato, "Cerebrovascular response to cognitive tasks and hyperventilation measured by multi-channel near-infrared spectroscopy," *J. Neuropsychiatry Clin. Neurosci.* **15**, 442–449 (2003).
 45. O. Spreen and E. A. Strauss, *Compendium of Neuropsychological Tests*, Oxford University Press, New York (1997).
 46. C. I. Elfgren and J. Risberg, "Lateralized frontal blood flow increases during fluency tasks: influence of cognitive strategy," *Neuropsychologia* **36**, 505–512 (1998).
 47. W. D. Gaillard, L. Hertz-Pannier, S. H. Mott, A. S. Barnett, D. LeBihan, and W. H. Theodore, "Functional anatomy of cognitive development: fMRI of verbal fluency in children and adults," *Neurology* **54**, 180–185 (2000).
 48. K. J. Friston, C. D. Frith, P. F. Liddle, and R. S. Frackowiak, "Investigating a network model of word generation with positron emission tomography," *Proc. R. Soc. London* **244**, 101–106 (1991).
 49. Y. Kitabayashi, H. Ueda, H. Tsuchida, H. Iizumi, J. Narumoto, K. Nakamura, H. Kita, and K. Fukui, "Relationship between regional cerebral blood flow and verbal fluency in Alzheimer's disease," *Psychiatry Clin. Neurosci.* **55**, 459–463 (2001).
 50. R. Schlosser, M. Hutchinson, S. Joseffer, H. Rusinek, A. Saarimaki, J. Stevenson, S. L. Dewey, and J. D. Brodie, "Functional magnetic resonance imaging of human brain activity in a verbal fluency task," *J. Neurol., Neurosurg. Psychiatry* **64**, 492–498 (1998).
 51. D. W. Dickins, K. D. Singh, N. Roberts, P. Burns, J. J. Downes, P. Jimmieson, and R. P. Bentall, "An fMRI study of stimulus equivalence," *NeuroReport* **12**, 405–411 (2001).
 52. W. D. Gaillard, B. C. Sachs, J. R. Whitnah, Z. Ahmad, L. M. Balsamo, J. R. Petrella, S. H. Braniecki, C. M. McKinney, K. Hunter, B. Xu, and C. B. Grandin, "Developmental aspects of language processing: fMRI of verbal fluency in children and adults," *Hum. Brain Mapp* **18**, 176–185 (2003).
 53. S. Abrahams, L. H. Goldstein, A. Simmons, M. J. Brammer, S. C. Williams, V. P. Giampietro, C. M. Andrew, and P. N. Leigh, "Functional magnetic resonance imaging of verbal fluency and confrontation naming using compressed image acquisition to permit overt responses," *Hum. Brain Mapp* **20**, 29–40 (2003).
 54. E. Gratton, S. Fantini, M. A. Franceschini, G. Gratton, and M. Fabiani, "Measurements of scattering and absorption changes in muscle and brain," *Phil. Trans. R. Soc. Lond. Biol. Sci.* **352**, 727–735 (1997).
 55. B. Chance, J. S. Leigh, H. Miyake, D. S. Smith, S. Nioka, R. Greenfield, M. Finander, K. Kaufmann, W. Levy, M. Young, P. Cohen, H. Yoshioka, and R. Boretski, "Comparison of time-resolved and -unresolved measurements of deoxyhemoglobin in brain," *Proc. Natl. Acad. Sci. U.S.A.* **85**, 4971–4975 (1988).
 56. D. T. Delpy, M. Cope, P. van der Zee, S. Arridge, S. Wray, and J. Wyatt, "Estimation of optical pathlength through tissue from direct time of flight measurement," *Phys. Med. Biol.* **33**, 1433–1442 (1988).
 57. A. Torricelli, V. Quaresima, A. Pifferi, G. Biscotti, L. Spinelli, P. Taroni, M. Ferrari, and R. Cubeddu, "Mapping of calf muscle oxygenation and haemoglobin content during dynamic plantar flexion exercise by multi-channel time-resolved near infrared spectroscopy," *Phys. Med. Biol.* **49**, 685–699 (2004).
 58. R. C. Haskell, L. O. Svaasand, T. T. Tsay, T. C. Feng, M. S. McAdams, and B. J. Tromberg, "Boundary conditions for the diffusion equation in radiative transfer," *J. Opt. Soc. Am. A* **11**, 2727–2741 (1994).
 59. Y. Nomura, O. Hazeki, and M. Tamura, "Relationship between time-resolved and non-time-resolved Beer-Lambert law in turbid media," *Phys. Med. Biol.* **42**, 1009–1023 (1997).
 60. R. Cubeddu, A. Pifferi, P. Taroni, A. Torricelli, and G. Valentini, "Experimental test of theoretical models for time-resolved reflectance," *Med. Phys.* **23**, 1625–1634 (1996).
 61. S. Prahl, Oregon Medical Laser Center website: <http://omlc.ogi.edu/spectra> (2001).
 62. R. C. Oldfield, "The assessment and analyses of handedness: the Edinburgh Inventory," *Neuropsychologia* **9**, 97–113 (1971).
 63. K. Audenaert, B. Brans, K. Van Laere, P. Lahorte, J. Versijpt, K. van Heeringen, and R. Dierckx, "Verbal fluency as a prefrontal activation probe: a validation study using 99mTc-ECD brain SPET," *Eur. J. Nucl. Med.* **27**, 1800–1808 (2000).
 64. I. Papousek and G. Schuster, "Manipulation of frontal brain asymmetry by cognitive tasks," *Brain Cogn.* **54**, 43–51 (2004).
 65. G. Vingerhoets and N. Stroobant, "Lateralization of cerebral blood flow velocity changes during cognitive tasks. A simultaneous bilateral transcranial Doppler study," *Stroke* **30**, 2152–2158 (1999).
 66. A. Seiyama, J. Seki, H. C. Tanabe, I. Sase, A. Takatsuki, S. Miyauchi, H. Eda, S. Hayashi, T. Imaruoka, T. Iwakura, and T. Yanagida, "Circulatory basis of fMRI signals: relationship between changes in the

- hemodynamic parameters and BOLD signal intensity," *Neuroimage* **21**, 1204–1214 (2004).
67. W. N. Colier, V. Quaresima, B. Oeseburg, and M. Ferrari, "Human motor-cortex oxygenation changes induced by cyclic coupled movements of hand and foot," *Exp. Brain Res.* **129**, 457–461 (1999).
 68. E. Okada and D. T. Delpy, "Near-infrared light propagation in an adult head model. II. Effect of superficial tissue thickness on the sensitivity of the near-infrared spectroscopy signal," *Appl. Opt.* **42**, 2915–2922 (2003).
 69. M. Okamoto, H. Dan, K. Sakamoto, K. Takeo, K. Shimizu, S. Kohno, I. Oda, S. Isobe, T. Suzuki, K. Kohyama, and I. Dan, "Three-dimensional probabilistic anatomical cranio-cerebral correlation via the international 10–20 system oriented for transcranial functional brain mapping," *Neuroimage* **21**, 99–111 (2004).
 70. G. Strangman, M. A. Franceschini, and D. A. Boas, "Factors affecting the accuracy of near-infrared spectroscopy concentration calculations for focal changes in oxygenation parameters," *Neuroimage* **18**, 865–879 (2003).
 71. J. Uludag, M. Kohl, J. Steinbrink, H. Obrig, and A. Villringer, "Cross talk in the Lambert-Beer calculation for near-infrared wavelengths estimated by Monte Carlo simulations," *J. Biomed. Opt.* **7**, 51–59 (2002).
 72. V. Quaresima, S. Sacco, R. Totaro, and M. Ferrari, "Non invasive measurement of cerebral hemoglobin oxygen saturation using two near infrared spectroscopy approaches," *J. Biomed. Opt.* **5**, 201–205 (2000).
 73. F. Vernieri, F. Tibuzzi, P. Pasqualetti, N. Rosato, F. Passarelli, P. M. Rossini, and M. Silvestrini, "Transcranial Doppler and near-infrared spectroscopy can evaluate the hemodynamic effect of carotid artery occlusion," *Stroke* **35**, 64–70 (2004).
 74. J. Choi, M. Wolf, V. Toronov, U. Wolf, C. Polzonetti, D. Hueber, L. P. Safonova, R. Gupta, A. Michalos, W. Mantulin, and E. Gratton, "Non invasive determination of the optical properties of adult brain: near-infrared spectroscopy approach," *J. Biomed. Opt.* **9**, 221–229 (2004).
 75. S. Del Bianco, F. Martelli, and G. Zaccanti, "Penetration depth of light re-emitted by a diffusive medium: theoretical and experimental investigation," *Phys. Med. Biol.* **47**, 4131–4144 (2002).
 76. J. Steinbrink, H. Wabnitz, H. Obrig, A. Villringer, and H. Rinneberg, "Determining changes in NIR absorption using a layered model of the human head," *Phys. Med. Biol.* **46**, 879–896 (2001).